Available online at www.sciencedirect.com
ScienceDirect
Journal of Molecular Catalysis A: Chemical 256 (2006) 164–170
JOURNAL OF MOLECULAR CATALYSIS A: CHEMICAL
www.elsevier.com/locate/molcata

One-step hydrogenolysis of dimethyl maleate to tetrahydrofuran over chromium-modified Cu–B/γ-Al_2O_3 catalysts

P.J. Guo, L.F. Chen, S.R. Yan, W.L. Dai, M.H. Qiao *, H.L. Xu, K.N. Fan *

Department of Chemistry and Shanghai Key Laboratory of Molecular Catalysis and Innovative Materials, Fudan University, Shanghai 200433, PR China

Received 25 January 2006; received in revised form 18 April 2006; accepted 20 April 2006
Available online 5 June 2006

Abstract

The one-step gas-phase hydrogenolysis of dimethyl maleate to tetrahydrofuran has been investigated over a series of chromium-modified Cu–B/γ-Al_2O_3 catalysts prepared by the wetness impregnation–chemical reduction method. The characterizations reveal that copper in the Cu–B/γ-Al_2O_3 and chromium-modified Cu–B/γ-Al_2O_3 catalysts is solely in the metallic state, while chromium and boron are in the oxidized state. The addition of chromium not only reduces the crystallite size of metallic copper and increases the dispersion, but also promotes the intrinsic activity of the Cu–B/γ-Al_2O_3 catalyst. With the aid of the acidity of γ-Al_2O_3, a tetrahydrofuran yield of 94% is achieved over the 30% Cr–Cu–B/γ-Al_2O_3 catalyst under optimized reaction condition.

Keywords: Cr–Cu–B; γ-Al_2O_3; Dimethyl maleate; Tetrahydrofuran; Hydrogenolysis

1. Introduction

The synthesis of tetrahydrofuran (THF) is of considerable interest due to its wide and important applications. THF is a precursor for polyurethanes, elastic fibers and molded elastomers copolyesters, and also finds widespread usage as high-performance solvent for many polymers. The expanding market for polytetramethylene ether glycol (PTMEG) with THF as monomer adds further demand for THF [1,2].

At present, the production of THF is dominated by the dehydration of 1,4-butanediol (BDO) which itself is manufactured by complicated routes or under stringent conditions [1,3]. A direct and selective route to THF is highly desirable considering the simplified operation procedures and conservation in energy. Recently, over an elaborately designed Cu/ZnO extrudate with γ-Al_2O_3 as a binder, Müller and coworkers achieved a nearly complete conversion of dimethyl maleate (DMM) to THF in single-stage gas-phase hydrogenolysis of DMM [4]. This route has additional merit as the polymeric deposits resulting from trans-esterification of BDO with DMM can be avoided due to the low concentration of BDO, which otherwise would plug the reactor during the operation [4,5].

On the other hand, unsupported ultrafine binary Cu–B and ternary M–Cu–B (M = Cr, Zn, La, V, Mn, Th) catalysts prepared by the chemical reduction method with borohydride as reductant are potential alternatives to Cu/Zn/Al_2O_3 and copper chromite catalysts which have found extensive usage in industrial hydrogenation processes including the hydrogenation of DMM and diethyl maleate [4–8]. Matsuda et al. demonstrated that the space yield of methanol on an ultrafine V–Cu–B catalyst was about 3.5 times as high as that on a co-precipitated Cu–Zn catalyst in liquid-phase hydrogenation of CO [9]. In the liquid-phase synthesis of methanol from CO_2 and H_2, Liaw and Chen found that an ultrafine 20% Zr–Cu–B catalyst was a good catalyst in the lower temperature range, while a 20% Cr–Cu–B catalyst was the better one in the range of 225–250 °C [10]. In another work [11], they systematically explored the hydrogenation of a series of organic molecules containing one or more olefinic and/or carbonyl groups over unsupported M–Cu–B catalysts, and suggested that a Cr–Cu–B catalyst (Cr < 5 mol%) could be a suitable candidate for the replacement of commercial copper chromite catalysts (Cr > 50 mol%).

Considering the superior activity of the Cr–Cu–B catalyst in saturating the olefinic and carbonyl groups, it is a natural extension to use such catalysts in the reaction of DMM hydrogenol-

* Corresponding authors. Tel.: +86 21 65643977; fax: +86 21 65642978.
E-mail addresses: mhqiao@fudan.edu.cn (M.H. Qiao), knfan@fudan.edu.cn (K.N. Fan).

1381-1169/$ – see front matter © 2006 Elsevier B.V. All rights reserved.
doi:10.1016/j.molcata.2006.04.047

ysis, as DMM molecules also have similar functional groups. Because γ-Al_2O_3 is indispensable for a high selectivity toward THF by providing the acid sites for BDO dehydration [4], in this paper we prepared a series of γ-Al_2O_3-supported Cr–Cu–B catalysts with different Cr contents and examined them in gas-phase hydrogenolysis of DMM in a fixed-bed reactor. Results demonstrated that the Cr-modified Cu–B/γ-Al_2O_3 catalyst is a promising alternative to the Cu/ZnO/γ-Al_2O_3 extrudates in one-step hydrogenolysis of DMM to THF.

2. Experimental

2.1. Catalyst preparation

The Cr-modified Cu–B/γ-Al_2O_3 samples were prepared by the following procedure. γ-Alumina (40–60 mesh, S_{BET} 136 $m^2\,g^{-1}$) was impregnated with a desired amount of mixed aqueous solution of $CuCl_2$ and $CrCl_3$ for 6 h at 303 K. The nominal copper loading was maintained at 10 wt.% relative to alumina. Then it was dried at 353 K with constant stirring, followed by drying at 373 K overnight to remove residual water. The precursor was reduced by adding 1.5 M aqueous solution of KBH_4 under vigorous stirring. The molar ratio of B/(Cu + Cr) was kept at 4/1 to ensure the reduction of the metal ions. The resulting black catalyst was washed with distilled water to neutrality, and then with methanol three times to replace water. The catalysts used for characterization were washed with ethanol instead of methanol. According to the chromium content, the catalysts were designated as *x*% Cr–Cu–B/γ-Al_2O_3, where *x* is the nominal molar percentage of Cr with respect to Cu in the preparation.

2.2. Catalyst characterization

The bulk composition was analyzed by inductively coupled plasma-atomic emission spectroscopy (ICP-AES; IRIS Intrepid). The Brunauer–Emmett–Teller surface area (S_{BET}) was measured using N_2 physisorption at 77 K on the Micromeritics TriStar3000 apparatus. Prior to measurement, the catalyst was transferred to the glass adsorption tube and degassed at 383 K under ultrahigh pure nitrogen flow for 2.0 h. The X-ray diffraction (XRD) pattern was collected on a Bruker AXS D8 Advance X-ray diffractometer using Cu Kα radiation (λ = 0.15418 nm). The tube voltage was 40 kV, and the current was 40 mA. A catalyst with solvent was put on the sample stage, with argon flow (99.9995%) purging the sample during the detection to avoid oxidation. The particle size and distribution were observed by transmission electron microscopy (TEM; JEOL JEM2011) which is equipped with an energy dispersive X-ray emission analyzer (EDX).

The surface species were detected by X-ray photoelectron spectroscopy (XPS; Perkin Elmer PHI5000C). The spectrum was recorded with Mg Kα line as the excitation source ($h\nu$ = 1253.6 eV). The sample was pressed to a self-supported disc and kept in ethanol before mounting on the sample plate. It was degassed in the pretreatment chamber at 383 K for 2 h in vacuo before being transferred into the analyzing chamber where the background pressure was lower than 2×10^{-9} Torr. All the binding energy (BE) values were referenced to the C 1s peak of contaminant carbon at 284.6 eV with an uncertainty of ±0.2 eV.

The active copper surface area was determined by temperature-programmed desorption of hydrogen (H_2-TPD). After treated at 523 K for 1 h under argon flow (99.9995%, deoxygenated by an Alltech Oxy-trap filter), the catalyst was cooled down to room temperature before saturation chemisorption of hydrogen by pulsed injection as confirmed by the constant eluted peak area. The maximum desorption temperature, 1000 K, was reached at a ramping rate of 20 K min^{-1}. The H_2 signal (mass 2) was monitored by an on-line mass spectrometer (MS; Stanford SRS200). Active surface area was calculated from the volume of hydrogen desorbed by assuming H/Cu(s) stoichiometry of unity and a value of 1.46×10^{19} Cu atoms per m^2 [12]. Turnover frequency (TOF) was expressed as the number of H_2 molecules consumed on per active surface copper atom per second during the reaction.

2.3. Activity test and product analysis

The catalytic experiments were carried out on a continuous flow unit equipped with a stainless-steel fixed-bed tubular reactor. The catalyst bed had a diameter of 11 mm and a length of approximately 30 mm. Both sides of the catalyst bed were packed with quartz powder (40–60 mesh) to ensure a plug flow profile of the feed. 20 vol.% DMM (purity > 98%) diluted with methanol and hydrogen were fed into the reactor at a H_2/DMM molar ratio varying from 80 to 140, and total pressure in the range of 3–6 MPa. The reaction temperatures were ranged from 493 to 563 K and the room-temperature space velocity (LSV) of DMM was set at 0.36 ml $(g_{cat.})^{-1}\,h^{-1}$. The products were condensed and analyzed by a gas chromatograph (Finnigan TraceGC ultra) fitted with an HP-5 capillary column and a flame ionization detector (FID).

3. Results and discussion

3.1. Chemical composition and surface area

The chemical composition and BET surface area of the Cr-modified Cu–B/γ-Al_2O_3 catalysts are summarized in Table 1. Chemical analysis reveals that on the Cu–B/γ-Al_2O_3 catalyst the copper loading is lower than the nominal amount, indicating that Cu has only been partly deposited on γ-Al_2O_3 using the chemical reduction method. The incorporation of Cr improves the copper loading to some extent, but excessive Cr reduces copper loading as for the 40% Cr–Cu–B/γ-Al_2O_3 catalyst. In these catalysts, the amount of Cr increases with Cr addition in the preparation, and is reasonably in close resemblance to the nominal value. Meanwhile, the presence of Cr promotes the co-precipitation of boron, which corroborates well by the observation by Chen et al. [10,11,13]. However, as compared to the ultrafine Cr–Cu–B catalysts, the amounts of Cr and B in the supported ones are much higher at the similar amount of Cr, which may be traced back to the very different reduction conditions between the two cases.

Table 1
Physico-chemical properties of the Cr-modified Cu–B/γ-Al_2O_3 catalysts

Sample	Cu loading[a] (wt.%)	Composition[b] (molar ratio)	Cr/Cu[c] (%)	S_{BET} ($m^2\ g^{-1}$)	d[d] (nm)	S_{Cu}[e] ($m^2\ g_{cat.}^{-1}$)
γ-Al_2O_3	–	–	–	136	–	–
Cu–B/γ-Al_2O_3	5.22	$Cu_{73.6}B_{26.4}$	–	123	18	4.9
10% Cr–Cu–B/γ-Al_2O_3	6.43	$Cu_{64.1}Cr_{10.1}B_{25.5}$	10.1	124	13	6.2
20% Cr–Cu–B/γ-Al_2O_3	6.26	$Cu_{54.5}Cr_{14.5}B_{31.0}$	16.7	130	13	6.4
30% Cr–Cu–B/γ-Al_2O_3	6.46	$Cu_{47.4}Cr_{20.2}B_{32.4}$	27.5	125	13	7.2
40% Cr–Cu–B/γ-Al_2O_3	4.87	$Cu_{34.5}Cr_{24.8}B_{40.7}$	35.0	126	12	6.7

[a] Cu loading relative to alumina.
[b] Oxygen and alumina are not included.
[c] The molar percentage of Cr in the catalyst relative to Cu in the preparation.
[d] Measured by TEM.
[e] Based on hydrogen desorption.

On the other hand, supporting of Cr–Cu–B on γ-Al_2O_3 does not alter the preliminary line-shape of the nitrogen physisorption isotherms of alumina, irrespective of the amount of chromium incorporated, although a slight drop in surface area has occurred (Table 1). It is a reflection of the low loading of Cr–Cu–B which does not remarkably block the pores of the support.

3.2. Crystalline phase and morphology

Fig. 1 shows the XRD patterns of Cu–B/γ-Al_2O_3 and 30% Cr–Cu–B/γ-Al_2O_3 as a representative for the Cr-modified catalysts. For both catalysts, besides the diffractions from γ-Al_2O_3 (JCPDS 46–1215), the diffractograms are dominated by the peaks at 2θ of 43.3°, 50.5° and 74.1°, which are assigned to (1 1 1), (2 0 0) and (2 2 0) planes of metallic Cu (JCPDS 04-0836), respectively. Like ultrafine Cu–B and Cr–Cu–B [10,11,13], no diffractions from Cr- and B-containing species are identified, possibly due to their small size beyond the detection limit of XRD and/or amorphous structure. Gaspar and Dieguez have prepared Cr/γ-Al_2O_3 catalysts with a Cr content comparable to our 30% Cr–Cu–B/γ-Al_2O_3 catalyst showing only diffraction peaks of γ-Al_2O_3, which is attributed to the strong interaction between Cr_2O_3 and γ-Al_2O_3 [14]. On the other hand, there is no diffraction peak from Cu_2O for the present Cu–B/γ-Al_2O_3 and Cr-modified Cu–B/γ-Al_2O_3 catalysts, which is different from the ultrafine Cu–B or Cr–Cu–B catalysts [10,11,13]. By XRD, it is difficult to discriminate the two situations whether there is really no Cu_2O or Cu_2O exists in high dispersion; however, XPS will demonstrate that metallic copper is the only Cu-containing species in the Cu–B/γ-Al_2O_3 and Cr-modified Cu–B/γ-Al_2O_3 catalysts.

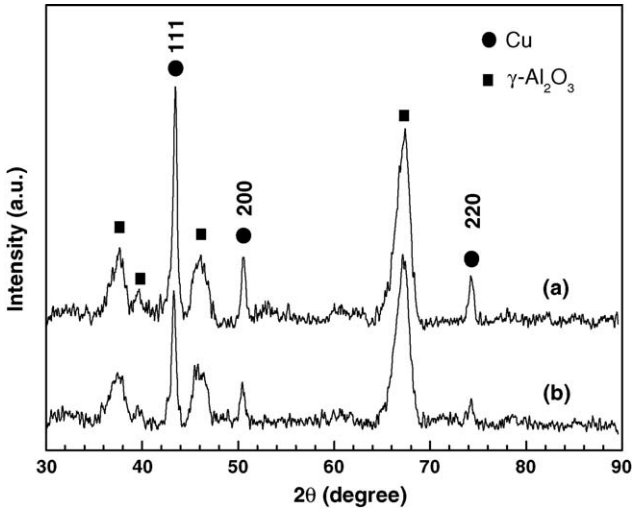

Fig. 1. XRD patterns of (a) Cu–B/γ-Al_2O_3 and (b) 30% Cr–Cu–B/γ-Al_2O_3 catalysts.

Further analysis of Fig. 1 reveals that the intensity ratio between metallic copper and γ-Al_2O_3 is much lower in Cr-modified Cu–B/γ-Al_2O_3 than in Cu–B/γ-Al_2O_3, suggesting that the incorporation of Cr improves the dispersion of copper, which is beneficial for promoting the activity of the Cu-based catalysts. Moreover, the diffraction peaks of metallic copper are broader after Cr incorporation. Based on the integral width of the Cu(1 1 1) diffraction line and the Scherrer relation, it is found that the mean size of the metallic copper crystallite is decreased from ca. 20 to 13 nm.

The increased dispersion and decreased crystallite size are directly confirmed by TEM. As shown in Fig. 2 and also listed in Table 1, the size of the metallic copper crystallites (with darker contrast as confirmed by EDX) is ∼18 nm in Cu–B/γ-Al_2O_3, and remains about 13 nm irrespective of the amount of Cr incorporated, which correlates well with the crystallite size estimated from X-ray line broadening. A similar phenomenon has been identified on Cr-modified Ni–B catalysts, which is attributed to the presence of oxidized Cr-containing species lowering the surface energy of the nanoparticles, thus impeding their aggregation [15]. EDX analysis further reveals that only a small portion of the incorporated Cr coexists with metallic copper crystallites, so most Cr should be highly dispersed on alumina surface, as suggested by the XRD results.

3.3. Surface species and chemical state

XPS analysis is carried out aiming to clarify the availability of Cu_2O and the chemical states of Cr and B on the catalysts, because XRD does not provide any information on these aspects. The Cu 2p spectra illustrated in Fig. 3a evidently exclude the existence of CuO, as evidenced by the absence of the Cu $2p_{3/2}$ peak at 932.6 eV and the 2p → 3d satellite at ∼943 eV characteristic of Cu^{2+} with electron configuration of d^9 [16,17].

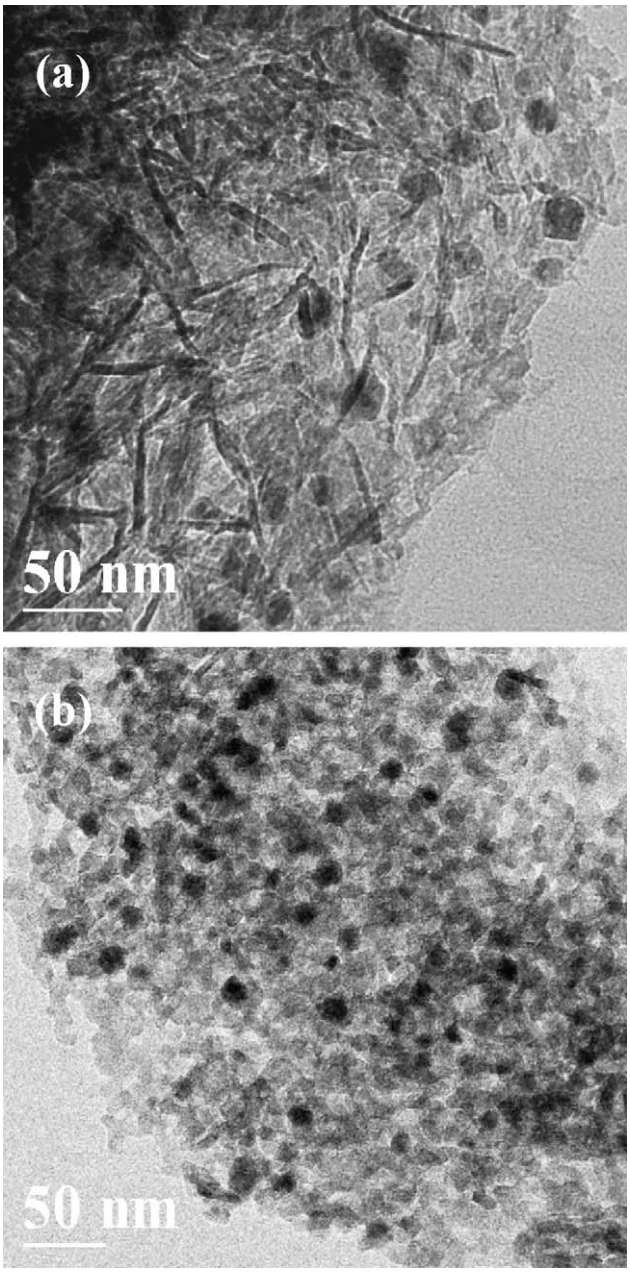

Fig. 2. TEM images of (a) Cu–B/γ-Al_2O_3 and (b) 30% Cr–Cu–B/γ-Al_2O_3 catalysts.

Combined with the Cu LMM kinetic energy (KE) of 918.0 eV (Fig. 3b), the presence of Cu_2O can also be excluded, as the modified Auger parameter (α') is 1850.6 eV, which is consistent with metallic copper rather than Cu_2O [18]. Thus in the Cu–B/γ-Al_2O_3 and Cr-modified Cu–B/γ-Al_2O_3 catalysts, copper is solely in its elemental state after the reduction by KBH_4.

In addition, the Cr 2p and B 1s spectra unambiguously confirm that Cr and B are in their oxidized states. In Fig. 3c, the Cr 2p spectrum for the Cr-modified Cu–B/γ-Al_2O_3 catalyst exhibits two peaks at 577.0 and 586.5 eV due to the Cr $2p_{3/2}$ and $2p_{1/2}$ levels of Cr_2O_3, respectively [16], suggesting that Cr^{3+} in $CrCl_3$ cannot be reduced by KBH_4, but hydrolyzes in basic KBH_4 solution. In Fig. 3d, the only one B 1s peak centered at 191.6 eV is unequivocally attributed to B_2O_3 [10,19].

3.4. Gas-phase hydrogenolysis of DMM

The effect of the amount of Cr on the catalytic behavior of the Cu–B/γ-Al_2O_3 catalysts in gas-phase hydrogenolysis of DMM has been investigated and the results are summarized in Table 2. Catalytic tests are conducted at reaction temperature of 533 K, total pressure of 5 MPa, H_2/DMM molar ratio of 120 and DMM LSV of 0.36 ml $(g_{cat.})^{-1}$ h^{-1}. Steady-state product compositions are obtained after ~8 h on stream. It is generally known that the hydrogenolysis of DMM proceeds via dimethyl succinate (DMS), γ-butyrolactone (GBL), and BDO, while BDO can dehydrate further to THF (Scheme 1) [4,5,20], which is found also being held on our Cu–B/γ-Al_2O_3 and Cr-modified Cu–B/γ-Al_2O_3 catalysts.

Since the hydrogenation of DMM to DMS is a very fast reaction [8], almost complete conversion of DMM (>97%) is observed over all the Cu–B/γ-Al_2O_3 and Cr-modified Cu–B/γ-Al_2O_3 catalysts, as listed in Table 2. Therefore, the conversion of DMS to subsequent products is adopted as a measure of the catalytic activity. In Table 2 one can find that Cr addition is beneficial for the hydrogenolysis of DMS. On the Cu–B/γ-Al_2O_3 catalyst, about 60.7 mol% of DMS remains intact, while DMS is decreased to 15.0 mol% on the 30% Cr–Cu–B/γ-Al_2O_3 catalyst. Excessive Cr is adverse to the catalytic activity, which results in the drop of the conversion of DMS at the Cr/Cu molar ratio of 40%.

According to XRD and TEM, the improved DMS conversion over the Cr-modified Cu–B/γ-Al_2O_3 catalysts than that over the unmodified Cu–B/γ-Al_2O_3 catalyst can be related to the reduced particle size and increased dispersion of metallic

Table 2
Effect of Cr modification on DMM hydrogenolysis at 533 K and 5 MPa[a]

Catalyst	Conversion (%)	Selectivity (%)				TOF ($\times 10^{-2}$ s^{-1})
		DMS	GBL	BDO	THF	
Cu–B/γ-Al_2O_3	97.3	62.4	15.2	3.9	18.5	2.9
10% Cr–Cu–B/γ-Al_2O_3	98.9	29.1	17.5	5.4	48.0	3.7
20% Cr–Cu–B/γ-Al_2O_3	99.3	27.2	18.4	4.7	49.7	3.7
30% Cr–Cu–B/γ-Al_2O_3	99.9	15.0	15.8	3.7	65.5	3.7
40% Cr–Cu–B/γ-Al_2O_3	98.3	19.6	14.1	3.8	62.5	3.8

[a] Other conditions: H_2/DMM (mol/mol) = 120, DMM LSV = 0.36 ml $(g_{cat.})^{-1}$ h^{-1}.

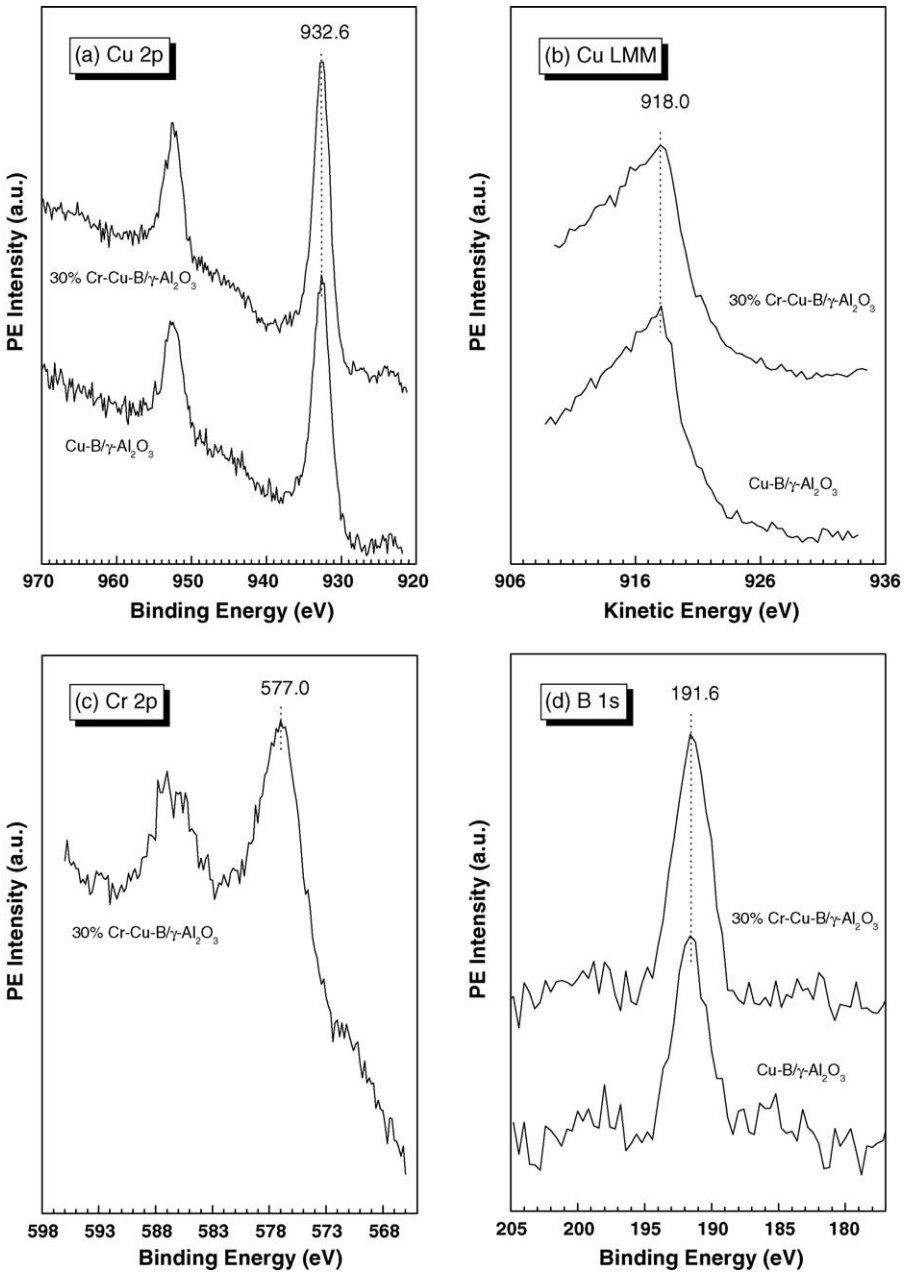

Fig. 3. XPS spectra of (a) Cu 2p, (b) Cu LMM, (c) Cr 2p, and (d) B 1s levels of the Cu–B/γ-Al_2O_3 and 30% Cr–Cu–B/γ-Al_2O_3 catalysts.

copper after Cr incorporation, thus exposing more active sites for DMM hydrogenolysis. Table 1 demonstrates that the active copper surface area per gram of catalyst exhibits the trend of Cu–B/γ-Al_2O_3 < 10% Cr–Cu–B/γ-Al_2O_3 < 20% Cr–Cu–B/γ-Al_2O_3 < 40% Cr–Cu–B/γ-Al_2O_3 < 30% Cr–Cu–B/γ-Al_2O_3, which is qualitatively in agreement with the evolution of DMS conversion over these catalysts. However, it is noted that the increment in the active surface area cannot fully account for

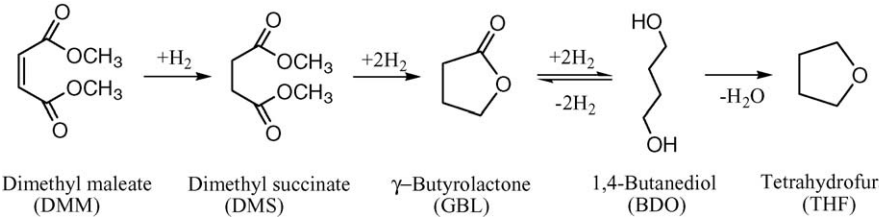

Scheme 1. Reaction scheme for the hydrogenolysis of dimethyl maleate to γ-butyrolactone, 1,4-butanediol and tetrahydrofuran.

the activity difference between the Cu–B/γ-Al_2O_3 and Cr-modified Cu–B/γ-Al_2O_3 catalysts, suggesting that chromium-modification has changed the nature of the Cu–B/γ-Al_2O_3 catalyst. The TOF values listed in Table 2 are in line with this deduction; the TOF of the Cu–B/γ-Al_2O_3 catalyst is 0.029 s^{-1}, while it is increased to around 0.037 s^{-1} for the Cr-modified Cu–B/γ-Al_2O_3 catalysts. As XPS reveals that the Cu $2p_{3/2}$ BEs of the Cu–B/γ-Al_2O_3 and Cr-modified Cu–B/γ-Al_2O_3 catalysts are identical, the modification of chromium on the electron structure of metallic copper seems unlikely to be the reason for the activity difference. In an additional experiment, we found that a Cu–B/γ-Al_2O_3 catalyst with lower Cu loading (~3 wt.%) and higher Cu dispersion has a TOF value similar to the present Cu–B/γ-Al_2O_3 catalyst, indicating that the changes in the TOF values of the Cu–B/γ-Al_2O_3 and Cr-modified Cu–B/γ-Al_2O_3 cannot be ascribed to the differences in Cu dispersion. It is possible that the oxidized chromium species promotes the intrinsic activity of the Cu–B/γ-Al_2O_3 catalyst by functioning as Lewis acid, which can activate the DMS molecule by polarizing the ester group. Such a mechanism has been employed in the interpretation of the promoting effect of some metal oxides including chromium on the hydrogenation of ketones and aldehydes over metal catalysts [21].

Aside from the activity difference, Table 2 shows that the Cu–B/γ-Al_2O_3 and Cr-modified Cu–B/γ-Al_2O_3 catalysts favor the formation of THF over that of GBL or BDO. For comparison, over a SiO_2-supported Cr–Cu–B catalyst prepared in a similar manner to the 30% Cr–Cu–B/γ-Al_2O_3 catalyst, GBL and BDO are the main products under the same reaction conditions. The discrepancy in product distribution can be ascribed to the weakly acidic γ-Al_2O_3 support which accelerates the dehydration of BDO to THF, shifting the equilibrium from GBL to BDO and consequently giving rise to a high selectivity toward THF, as suggested by Müller et al. for their extruded Cu–ZnO/γ-Al_2O_3 catalyst [4]. Moreover, it is found that chromium significantly enhances the selectivity to THF. When the nominal Cr/Cu molar ratio increases from 0 to 30%, the selectivity to THF increases drastically from 18.5 to 65.5%. Again, the THF selectivity declines when the Cr/Cu ratio is raised to 40%. The coincidence in the trends of the catalytic activity and the selectivity to THF on the Cu–B/γ-Al_2O_3 and Cr-modified Cu–B/γ-Al_2O_3 catalysts implies that the dehydration activity of γ-Al_2O_3 surpasses the hydrogenation activity of Cu–B and Cr-modified Cu–B, and that the formation of THF is limited by the hydrogenation activity of the catalysts.

Since the 30% Cr–Cu–B/γ-Al_2O_3 catalyst exhibits superior activity and selectivity in hydrogenolysis of DMM to THF, the reaction conditions are optimized to obtain higher selectivity and yield of THF, as illustrated in Fig. 4. Fig. 4a shows the effect of system pressure on the distribution of the hydrogenolysis products. It is found that when the pressure is doubled from 3.0 to 6.0 MPa, the selectivity to BDO remains at a low level, which is consistent with the relatively higher dehydration activity than the hydrogenation activity of the catalyst. In contrast, the selectivity to THF increases almost linearly at the expense of DMS and GBL. As is expected, a higher operation pressure enhances the hydrogenolysis reaction [5,20], which is the prerequisite

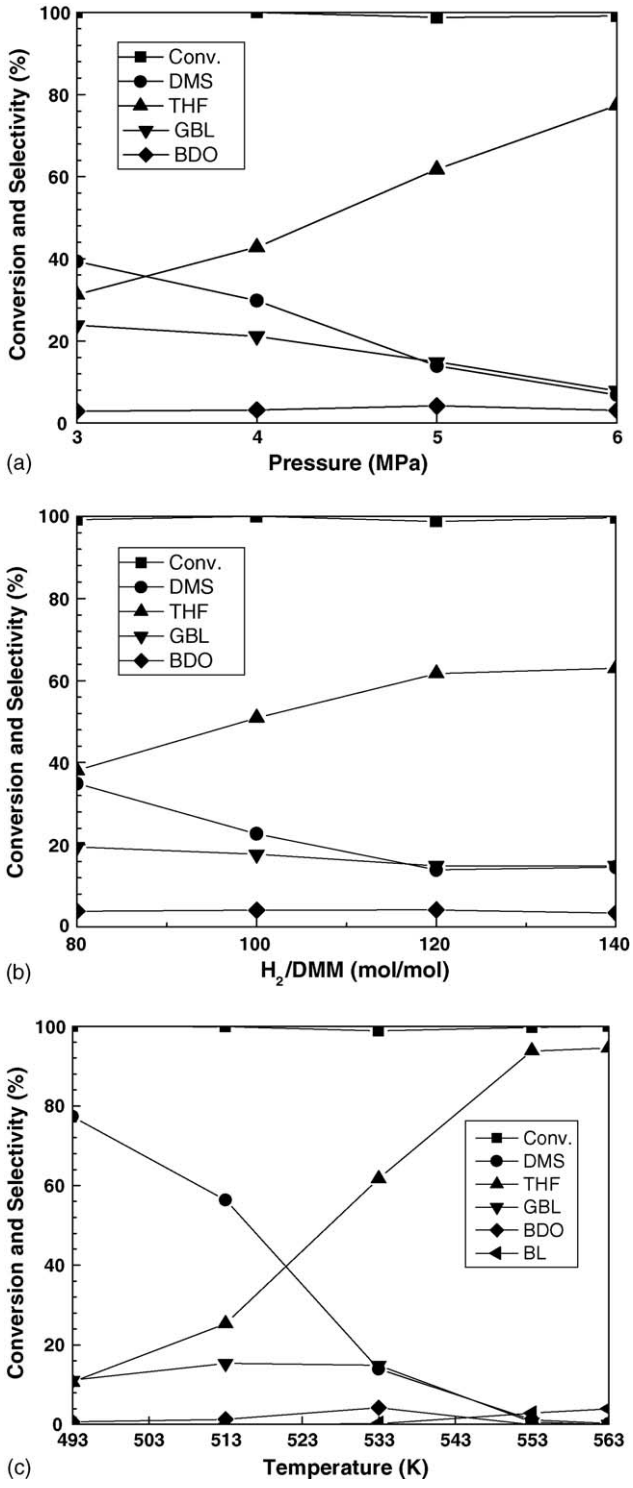

Fig. 4. Effect of reaction conditions on the hydrogenolysis of DMM over the 30% Cr–Cu–B/γ-Al_2O_3 catalyst. Other conditions: (a) T = 533 K, H_2/DMM = 120 (mol/mol), DMM LSV = 0.36 ml $(g_{cat.})^{-1}$ h^{-1}, (b) T = 533 K, p = 5 MPa, DMM LSV = 0.36 ml $(g_{cat.})^{-1}$ h^{-1}, and (c) p = 5 MPa, H_2/DMM = 120 (mol/mol), DMM LSV = 0.36 ml $(g_{cat.})^{-1}$ h^{-1}.

for the successive dehydration reaction. Fig. 4b shows that the THF selectivity can be improved only when the H_2/DMM ratio increases from 80 to 120. Further increase in this ratio does not significantly influence the performance of the catalyst. As far as

the operation economy is concerned, a H_2/DMM ratio of 120 is appropriate for THF production.

As to the effect of reaction temperature, Fig. 4c shows that when the temperature increases from 493 to 553 K, the THF selectivity increases, while DMS, GBL, and BDO virtually diminish. It seems that at higher reaction temperatures, the hydrogenation activity matches well with the dehydration activity, thus leading to a higher selectivity toward THF. At 553 K, a THF selectivity as high as 94% is obtained at the complete conversion of DMM. 1-Butanol (BL) is the only byproduct that limits the total formation of THF. Even higher temperatures do not favor the formation of THF, as BL increases much more rapidly than THF. In separate experiments, we find that when SiO_2, ZrO_2, TiO_2, or MgO is used as the support for Cr–Cu–B, the optimized THF selectivity is ∼80% at most, which may be ascribed to their inferior dehydration ability to γ-Al_2O_3. According to Fig. 4c, the dehydration rate of BDO to THF is faster than the hydrogenolysis rate of DMM to BDO on the 30% Cr–Cu–B/γ-Al_2O_3 catalyst, as manifested by the low concentration of BDO throughout the temperature range being investigated. It strongly suggests that the dehydration activity of the γ-Al_2O_3 support is sufficient for converting immediately the produced BDO to THF. Thus in order to further improve the selectivity to THF, the low-temperature hydrogenolysis activity of the catalyst should be enhanced to avoid the formation of BL which is favored at high temperature. Such work is being carried out in our laboratory.

4. Conclusions

The Cr-modified Cu–B/γ-Al_2O_3 catalysts are effective in one-step hydrogenolysis of DMM to THF with high selectivity. A suitable amount of chromium improves the dispersion of the catalyst and enhances the intrinsic catalytic activity. Besides, the acidic γ-Al_2O_3 support ensures the high selectivity toward THF. Over the 30% Cr–Cu–B/γ-Al_2O_3 catalyst, a THF yield of 94% is obtained under the optimized reaction conditions, with the main side product being 1-butanol.

Acknowledgments

This work was supported by the State Key Basic Research Development Program (G2000048009), the National Natural Science Foundation of China (20203004) and Shanghai Science and Technology Committee (03QB14004).

References

[1] K. Weissermel, H.J. Arpe, Industrial Organic Chemistry, 3rd ed., Wiley–VCH, Weinheim, 1997.
[2] H. Müller, Industrial Organic Chemicals: Starting Materials and Intermediates (Ullmann's Encyclopedia), vol. 8, Wiley–VCH, Weinheim, 1999, p. 4621.
[3] T. Haas, B. Jaeger, R. Weber, S.F. Mitchell, C.F. King, Appl. Catal. A 280 (2005) 83.
[4] S.P. Müller, M. Kucher, C. Ohlinger, B. Kraushaar-Czarnetzki, J. Catal. 218 (2003) 419.
[5] C. Ohlinger, B. Kraushaar-Czarnetzki, Chem. Eng. Sci. 58 (2003) 1453.
[6] M.A. Wood, P. Willett, D.M. Sutton, J. Ladebeck, Shokubai 40 (1998) 298.
[7] Q. Zhang, Z. Wu, L. Xu, Ind. Eng. Chem. Res. 37 (1998) 3525.
[8] M. Mokhtar, C. Ohlinger, J.H. Schlander, T. Turek, Chem. Eng. Technol. 24 (2001) 4.
[9] T. Matsuda, M. Shizuta, J. Yoshizawa, E. Kikuchi, Appl. Catal. A 125 (1995) 293.
[10] B.J. Liaw, Y.Z. Chen, Appl. Catal. A 206 (2001) 245.
[11] B.J. Liaw, Y.Z. Chen, Appl. Catal. A 196 (2000) 199.
[12] J.W. Evans, M.S. Wainwright, A.J. Bridgewater, D.J. Young, Appl. Catal. 7 (1983) 75.
[13] Y.Z. Chen, B.J. Liaw, B.J. Chen, Appl. Catal. A 236 (2002) 121.
[14] A.B. Gaspar, L.C. Dieguez, J. Catal. 220 (2003) 309.
[15] J. Fang, X.Y. Chen, B. Liu, S.R. Yan, M.H. Qiao, H.X. Li, H.Y. He, K.N. Fan, J. Catal. 229 (2005) 97.
[16] Handbook of X-ray Photoelectron Spectroscopy, Perkin Elmer Corporation, 1992.
[17] L. Meda, G.F. Cerofolini, Surf. Interface Anal. 36 (2004) 756.
[18] J. Morales, A. Caballero, J.P. Holgado, J.P. Espinós, A.R. González-Elipe, J. Phys. Chem. B 106 (2002) 10185.
[19] X.Y. Chen, S. Wang, J.H. Zhuang, M.H. Qiao, K.N. Fan, H.Y. He, J. Catal. 227 (2004) 419.
[20] J.H. Schlander, T. Turek, Ind. Eng. Chem. Res. 38 (1999) 1264.
[21] P. Gallezot, D. Richard, Catal. Rev. Sci. Eng. 40 (1998) 81.